

Design of the Signal Generator for ISS-Bioreactor

Aykut C. Satici*

Boise State University

Mechanical and Biomedical Engineering

(Dated: April 17, 2023)

This technical report is prepared to document the design of the signal generator circuit for the ISS-Bioreactor project at Boise State University.

1. INTRODUCTION

We design an input PWM filter to create the desired 0–10V sine wave at 90Hz that the controller expects from a carrier PWM signal at a carrier frequency 36.6kHz.

This technical report builds the final design up over a few major steps. For the impatient reader, the theoretical analysis, the implementation, and the full blown-up schematic of the final design are provided in Section 2.3, Section 3, and Figure 9 of the Appendix A, respectively.

2. THEORETICAL ANALYSIS

We perform a basic PWM filter design to generate the driving 0–10V sine wave signal to be fed into the Physik Instrumente (PI)’s controller for one of their piezoelectric actuators [2].

2.1. Basic Lowpass Filter Design

Consider the first-order filter sketched in Figure 1 with a sinusoidal driving voltage. The current i over the capacitor is $i = C \frac{dv_o}{dt}$. KVL around the loop gives

$$RC \frac{dv_o}{dt} + v_o = v_{\text{sig}} = A \cos(\omega t)$$

This differential equation has the transfer function

$$G(s) = \frac{1}{RCs + 1}.$$

The steady-state solution of the differential equation is obtained as

$$\begin{aligned} v_o(t) &= A |G(j\omega)| \cos(\omega t + \angle G(j\omega)) \\ &= \frac{A}{\sqrt{1 + \omega^2 R^2 C^2}} \cos(\omega t - \arctan(\omega RC)) \end{aligned}$$

Since we do not want our signal to be attenuated by the low-pass filter, we must choose the values of R and C such that $\omega RC \ll 1$ or $2\pi RC \ll 1/f$.

Unfortunately, our actual input from the microcontroller is not a pure sine wave, rather a PWM signal. Therefore, we also need the value of $2\pi RC$ to be large so that it attenuates the high frequencies present in the

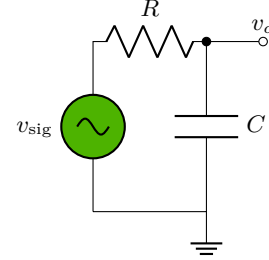


FIG. 1: A first-order low-pass filter circuit.

PWM signal. This requirement is difficult to achieve with just a first-order low-pass filter, leading us to design a second-order low-pass filter in the next subsections.

2.2. Second-Order LPF Design

A second-order filter is implemented as a linear operator from the Teensy-generated PWM voltage input v_t to the voltage v_i , as presented in Figure 2. The remainder of this circuit constitutes a noninverting op-amp that amplifies the sine wave extracted from its PWM modulation from 0–3.3V to 0–10V. We analyze the circuit so as to figure out the values of the various resistances and capacitances.

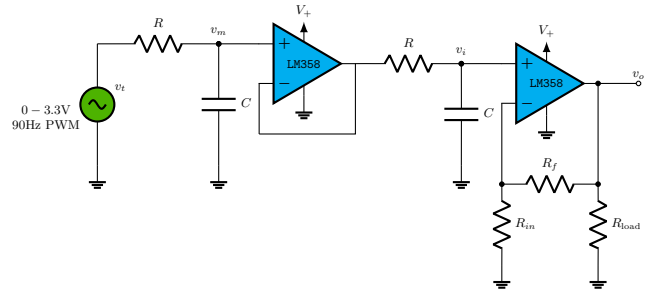


FIG. 2: The signal generator circuit.

The 0–3.3V PWM signal is to be filtered to extract the modulated sine wave. Thanks to the buffer op-amp, the transfer function from the Teensy input v_t to the input v_i to the non-inverting amplifier op-amp is given by

$$H(s) = \frac{V_i(s)}{V_t(s)} = \frac{1}{R^2 C^2 s^2 + 2RCs + 1}.$$

This is a critically-damped transfer function with both

*Electronic address: aykutsatici@boisestate.edu

poles at $s_{1,2} = -1/RC$. In other words, the cut-off frequency of this filter is at $f_n = \frac{1}{2\pi RC}$ with a roll-off of 40dB per decade. Contrast this to the first-order filter of the previous subsection where the roll-off was 20dB per decade. The greater roll-off rate allows us to be able to select $2\pi RC \ll 1/f$ while simultaneously achieving excellent high-frequency attenuation.

Our desired signal is a 90Hz sinusoidal, which should not be attenuated by the low-pass filter, i.e., the transfer function $H(s)$ should have approximately a unity gain at this frequency. To that end, we set $f_n = 5 \times 90 = 450\text{Hz}$, which produces the constraint $RC \leq 1/2\pi f_n$.

The attenuation needed at the PWM carrier frequency $f_c = 36.6\text{kHz}$ provides us with a lower bound on the product RC . If we want no less than α -fold attenuation, then we must have that

$$\begin{aligned} -20 \log \alpha &\geq 20 \log |H(j2\pi f_c)| = -20 \log (1 + 4\pi^2 R^2 C^2 f_c^2) \\ \Rightarrow 1 + 4\pi^2 R^2 C^2 f_c^2 &\geq \alpha \Rightarrow RC \geq \frac{\sqrt{\alpha - 1}}{2\pi f_c}. \end{aligned}$$

We summarize the lower and upper bounds on RC :

$$\frac{\sqrt{\alpha - 1}}{2\pi f_c} \leq RC \leq \frac{1}{2\pi f_n}.$$

Lastly, we want to amplify the input voltage v_i thrice in order to hit the 0 – 10V mark. The gain of the non-inverting amplifier is $k = 1 + R_f/R_{in}$. We choose $R_f, R_{in} \geq 1\text{k}\Omega$ so as to achieve $k = 3$. The high gain bandwidth product of the LM358 op-amp is read from its datasheet to be $\text{GBP} = 1.2\text{MHz}$. Hence the transfer function from the input voltage v_i to the output voltage v_o that will be applied to the PI controller is approximately given by

$$\frac{V_o(s)}{V_i(s)} = \frac{k}{\frac{k}{2\pi \text{GBP}} s + 1} \approx \frac{3}{3.979 \times 10^{-7} s + 1},$$

which will have a firm unity gain at our desired oscillation frequency of 90Hz.

2.3. Sallen-Key Architecture

Another well-known architecture that works well for this sort of problem is the Sallen-Key low-pass filter, which replaces the two RC +buffer combination whose output enters the amplifier op-amp, as shown in Figure 3. The blown-up full schematic of signal generator circuit may be found in Figure 9 of the appendix.

We find the governing equations of this circuit. Assume an ideal op-amp model so that both of the inputs of the op-amp have potential v_i . Let the current i flowing over R_1 split into i_1 and i_2 , the former flowing into C_1 and the latter into C_2 through R_2 . KCL gives

$$\begin{aligned} i &= i_1 + i_2 = \frac{1}{R_1}(v_t - v_m), \\ i_1 &= C_1 \frac{d(v_m - v_i)}{dt}, \\ i_2 &= C_2 \frac{dv_i}{dt}. \end{aligned}$$

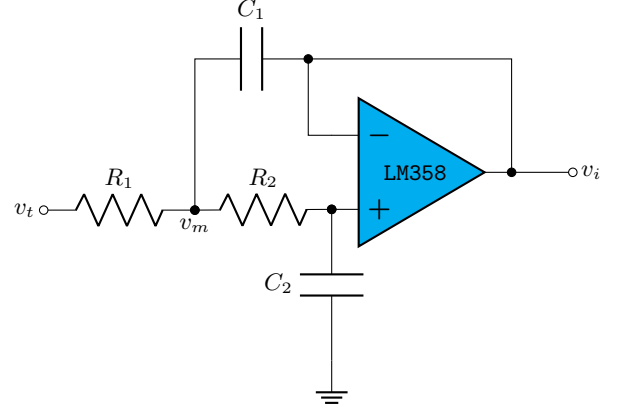


FIG. 3: Sallen Key (second-order) low-pass filter.

KVL around the bottom loop ($v_m - v_i - \text{gnd}$) gives $v_m = R_2 i_2 + v_i = R_2 C_2 \frac{dv_i}{dt} + v_i$. Plugging this into the second equation gives $i_1 = R_2 C_1 C_2 \frac{d^2 v_i}{dt^2}$. Combined with the first and third equations, this yields

$$R_1 R_2 C_1 C_2 \ddot{v}_i + (R_1 + R_2) C_2 \dot{v}_i + v_i = v_t. \quad (1)$$

The transfer function of the Sallen-Key filter is read as

$$T(s) = \frac{1}{R_1 R_2 C_1 C_2 s^2 + (R_1 + R_2) C_2 s + 1}. \quad (2)$$

The gain and phase of this transfer function may be computed as follows

$$\begin{aligned} |T(j\omega)| &= \frac{1}{\sqrt{1 + R_1^2 R_2^2 C_1^2 C_2^2 \omega^4}}, \\ \angle T(j\omega) &= -\arctan \frac{(R_1 + R_2) C_2 \omega}{1 - R_1 R_2 C_1 C_2 \omega^2}. \end{aligned} \quad (3)$$

We want to make this a Butterworth filter, making its frequency response as flat as possible in the passband. To that end, we identify the characteristic polynomial as

$$s^2 + \frac{R_1 + R_2}{R_1 R_2 C_2} s + \frac{1}{R_1 R_2 C_1 C_2} = s^2 + 2\zeta\omega_n s + \omega_n^2,$$

with the damping coefficient $\zeta = 1/\sqrt{2}$. This requirement on the damping coefficient translates to the constraint on the circuit elements:

$$\frac{(R_1 + R_2)^2}{2R_1 R_2} = \frac{C_1}{C_2}. \quad (4)$$

This Butterworth filter requirement simplifies the gain and phase (3) of the transfer function (2) as

$$\begin{aligned} |T(j\omega)| &= \frac{1}{\sqrt{1 + 1/4(R_1 + R_2)^4 C_2^4 \omega^4}}, \\ \angle T(j\omega) &= -\arctan \frac{2(R_1 + R_2) C_2 \omega}{2 - (R_1 + R_2)^2 C_2^2 \omega^2}. \end{aligned} \quad (5)$$

We ask that the magnitude of the output signal to be very close to the input signal, i.e., $1/\alpha_1 |v_t(t)| \leq |v_i(t)| \leq |v_t(t)|$ at the frequency of operation f_o (e.g. 90Hz), where $\alpha_1 > 1$ and $\alpha_1 \approx 1$ (e.g. $\alpha_1 = 1 + 1/1000$).

$$\sqrt{1 + 1/4(R_1 + R_2)^4 C_2^4 (2\pi f_o)^4} \leq \alpha_1,$$

or solving for the circuit elements

$$(R_1 + R_2)C_2 \leq \frac{\sqrt[4]{\alpha_1^2 - 1}}{\sqrt{2\pi f_o}}. \quad (6)$$

Asking for no less than α_2 -fold attenuation ($\alpha_2 \gg 1$) at the PWM carrier frequency f_c provides the constraint

$$\sqrt{1 + 1/4(R_1 + R_2)^4 C_2^4 (2\pi f_c)^4} \geq \alpha_2,$$

or, solving for the circuit elements,

$$(R_1 + R_2)C_2 \geq \frac{\sqrt[4]{\alpha_2^2 - 1}}{\sqrt{2\pi f_c}}. \quad (7)$$

Combining the gain requirements (6) and (7), we obtain the design interval

$$\frac{\sqrt[4]{\alpha_2^2 - 1}}{\sqrt{2\pi f_c}} \leq (R_1 + R_2)C_2 \leq \frac{\sqrt[4]{\alpha_1^2 - 1}}{\sqrt{2\pi f_o}}. \quad (8)$$

To find specific values for the resistances and capacitances, we specify the following quantities:

1. Tolerated attenuation at operation frequency: α_1 ,
2. The value of the decoupling capacitance: C_2 ,
3. The ratio between the resistances: $r = R_1/R_2$.

Once these are specified, the values of the remaining circuit components can be pinpointed. Indeed, from the constraint (4), we obtain that

$$C_1 = \frac{(1+r)^2}{2r} C_2.$$

We make sure that the signal amplitude is attenuated no more than a factor of α_1 at the operating frequency as well as provides ample attenuation at the PWM carrier frequency by satisfying the second inequality in (8) as equality. This gives

$$R_2 = \frac{\sqrt[4]{\alpha_1^2 - 1}}{(1+r)\sqrt{2\pi C_2}} \quad \text{and} \quad R_1 = rR_2.$$

Remark 1. Choosing the values for the circuit elements in this manner also determines the natural frequency and hence the phase shift. From the Sallen-Key filter transfer function 2, the natural frequency is computed as

$$f_n = \frac{1}{2\pi\sqrt{R_1 R_2 C_1 C_2}} = \frac{f_o}{\sqrt[4]{\alpha_1^2 - 1}}.$$

Further, using equation (5), the phase shift is given by

$$\angle T(j2\pi f) = -\arctan \frac{\sqrt{2}f/f_n}{1 - f^2/f_n^2}.$$

TABLE I: Theoretical values of resistances and capacitances.

R_1	R_2	C_1	C_2	R_f	R_{in}
440.8k Ω	88.2k Ω	3.6nF	1nF	2k Ω	1k Ω

We have used this procedure to compute the values for the circuit components, selecting $\alpha_1 = 1 + 1/1000$, $C_2 = 1\text{nF}$ and $r = 5$. The values for the remaining components are provided in Table I. This is a Butterworth filter that is maximally flat in its passband with $f_n = 425.5\text{Hz}$ and provides -77.4dB attenuation at the carrier frequency. At the operation frequency $f_o = 90\text{Hz}$, this filter introduces a phase shift of -17.39° .

Remark 2. This is the filter to be implemented in the final design. The experimental values of R_1 , R_2 , C_1 and C_2 are selected to be standard values that are closest to the values provided in Table I.

3. RESULTS

We provide extensive simulation and experimental data and their interpretation, supporting that the proposed analog signal generator works as intended.

3.1. Simulation

We perform a realistic LTSpice [1] simulation of both second-order filters derived in Sections (2.2, 2.3). One of the important aspects of these designs is the selection of the op-amp. In order to keep the common-mode voltage at 0V we choose the op-amps as CMOS type. One such op-amp is LM358 [4], which is used in the final design, even though a similar op-amp OP292 was used in this simulation.

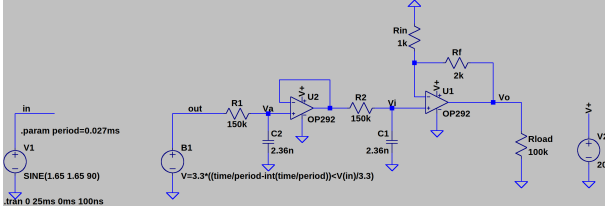
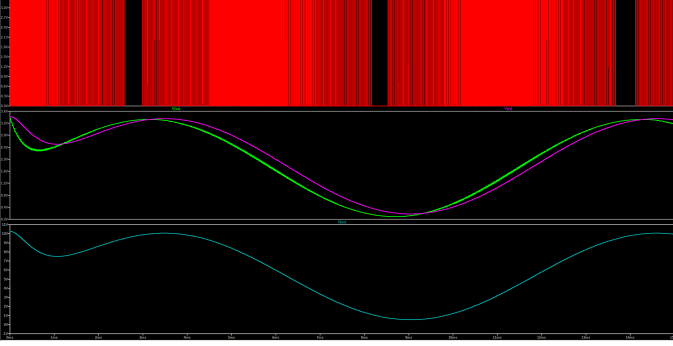
The PWM signal generated by Teensy [3] is simulated with a carrier frequency of 36.6kHz modulating the signal

$$V_{\text{pwm}} = 3.3/2 + 3.3/2 \sin(2\pi 90t).$$

Finally, the impedance of the load (PI's controller) is read off from its datasheet and inserted as a 100k Ω resistance.

3.1.1. RC+Buffer Simulation

The simulation for the architecture in Section 2.2 generates the relevant voltage responses, provided in Figure 5. The top plot shows the PWM signal generated by Teensy modulating a sine-wave at 90Hz frequency. The individual plots in the middle show the output of the first (green) and the second (purple) RC low-pass filters (v_m and v_i in Figure 2, respectively) that extract the modulated signal from its PWM representation. Finally, the last plot shows the thrice amplified signal through the op-amp OP292. The simulated circuit is provided in Figure 4.

FIG. 4: The RC +buffer signal generator circuit in LTSpice.FIG. 5: The response of the RC +buffer signal generator.

3.1.2. Sallen-Key Simulation

The performance of the Sallen-Key architecture from Section 2.3 is shown in Figure 6. The values for the resistances were taken to be $R_1 = 416.8k\Omega$, $R_2 = 83.4k\Omega$, $R_f = 2R_{in} = 1k\Omega$ and capacitances to be $C_1 = 3.6nF$, $C_2 = 1nF$. The LTSpice circuit diagram for this simulation is provided in Figure 7. Even though the performance of the Sallen-Key filter of Section 2.3 looks very similar to the RC +buffer filter of Section 2.2 in simulation, the experiments favor the Sallen-Key significantly. We will implement this filter in our final design.

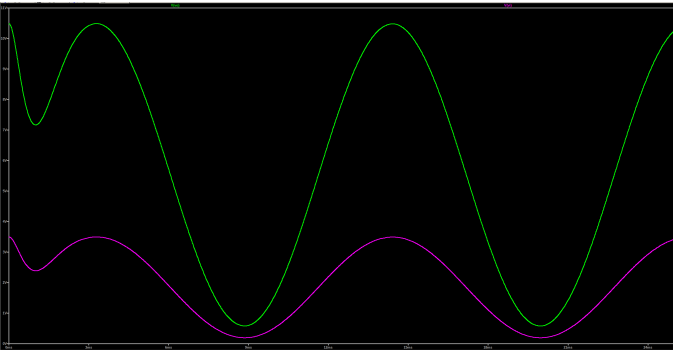


FIG. 6: The response of the Sallen-Key architecture.

3.2. Experiment

The Sallen-Key architecture is implemented on a simple setup on my tabletop. A snapshot of Teensy's PWM signal that modulates the desired sine-wave output is provided in Figure 8a.

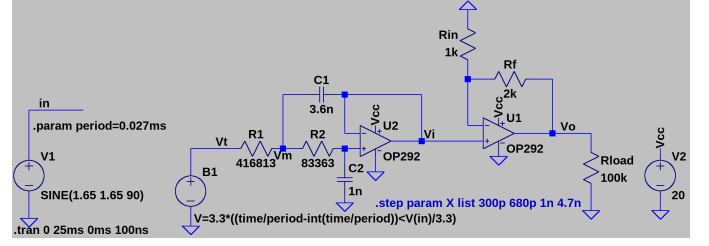
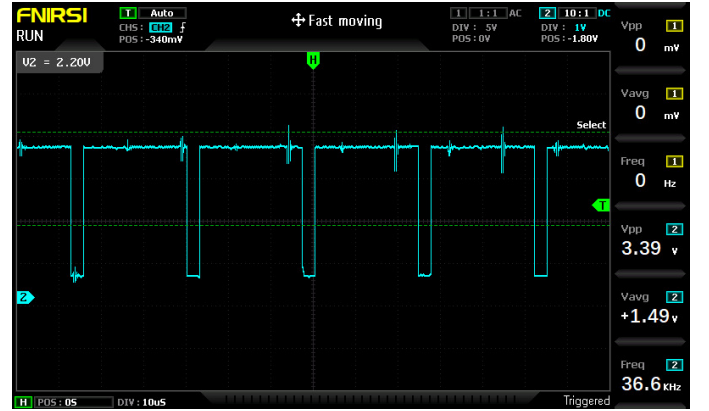
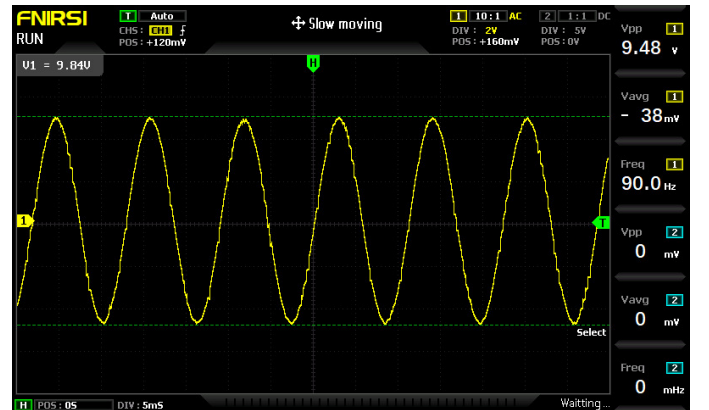


FIG. 7: The Sallen-Key filter circuit in LTSpice.

Figure 8b shows the response of the second-order Sallen-Key LPF observed through an oscilloscope. This is the output of the signal generator in response to the Teensy generated 90Hz 0–3.3V PWM signal modulating the desired sine wave. This response is satisfactory and should drive the PI controller without any issues.



(a) A snapshot of Teensy's PWM signal with a carrier frequency of 36.6kHz.



(b) The response of the second-order Sallen-Key filter.

FIG. 8: Experimental verification of the Sallen-Key filter design.

We have also tested the signal generator by driving PI's piezoelectric actuator. It turns out that since Teensy's imperfect PWM generation, the best values of the various capacitances and resistances seen in the circuit diagram 9 are as given in Table II. These are the values to be used

TABLE II: Experimental values of resistances and capacitances.

R_1	R_2	C_1	C_2	R_f	R_{in}
500k Ω	100k Ω	3.20nF	1nF	2k Ω	1k Ω

in the final design.

4. DISCUSSION AND CONCLUSIONS

A sine wave is modulated using a 0–3.3V PWM output of a Teensy 4.1 microcontroller at a carrier frequency of 36.6kHz. We presented two second-order lowpass filters to extract the modulated signal from its PWM represen-

tation: (i) RC +buffer configuration, (ii) Sallen-Key architecture. We have shown that in simulation both filters perform similarly, however in experiments the Sallen-Key filter performs significantly better. We have decided to use this filter in our final design on the bioreactor.

5. ACKNOWLEDGMENT

The author thanks Drs. John Chiasson and Vishal Saxena of Electrical and Computer Engineering at Boise State University and University of Delaware, respectively, for their invaluable insights into the practical implementation of the signal generator.

-
- [1] Analog Devices. LTSpice. URL <https://www.analog.com/en/design-center/design-tools-and-calculators/ltspice-simulator.html>.
[2] Physik Instrumente. E-610. URL <https://www.physikinstrumente.com/en/products/controllers-and-drivers/nanopositioning-piezo-controllers/e-610-piezo-amplifier-controller-601000>.
[3] PJRC. Teensy. URL <https://www.pjrc.com/teensy/>.
[4] Texas Instruments. LM358B. URL <https://www.ti.com/product/LM358B>.

Appendix A: Full Circuit Drawing of the Final Design

The final signal generator circuit schematic is presented in Figure 9. The potential v_t denotes the 0–3.3V PWM signal modulating a 90Hz sinusoidal wave at a carrier frequency of 36.6kHz. The potential v_o denotes the 0–10V analog 90Hz sine-wave signal ready to be sent to the Physik Instrumente controller E-610, depicted in the figure as the impedance R_{load} , as its reference input. The capacitances and the resistances are provided in Table II.

Appendix B: Alternative Filter

During testing, I have mistakenly implemented the circuit presented in Figure 10. Later, I analyzed the circuit by figuring out its transfer function. I include this circuit in here just as an academic curiosity. It has no bearing on the ISS mission and should be ignored for that purpose.

1. Deriving the equations of the circuit

The voltage divider at the inverting input of the second op-amp gives

$$v_o = (1 + R_f/R_{in}) v_i =: k v_i. \quad (B1)$$

Let i_1 and i_2 be the currents that flow over C_1 and C_2 , respectively. KVL around various loops give the following

relationships

$$v_m = R_2 i_2 + v_i, \quad (v_m - v_i - \text{gnd}), \quad (B2)$$

$$v_m = R i_1 + v_1 + v_i, \quad (v_m - v_1 - v_i - \text{gnd}), \quad (B3)$$

$$v_t = R_1 (i_1 + i_2) + v_m, \quad (v_t - v_m - \text{gnd}). \quad (B4)$$

The constitutive equations for capacitors provide the last two relevant equations

$$i_1 = C_1 \dot{v}_1, \quad i_2 = C_2 \dot{v}_i.$$

We want to obtain an input-output relationship between v_t and v_o .

a. Step 1. Use constitutive equations for the capacitors to reduce equations (B2–B4).

$$\begin{aligned} v_m &= R_2 C_2 \dot{v}_i + v_i = R C_1 \dot{v}_1 + v_1 + v_i, \\ v_t &= R_1 C_1 \dot{v}_1 + R_1 C_2 \dot{v}_i + v_m. \end{aligned}$$

b. Step 2. Substitute equation (B2) into equation (B4).

$$\begin{aligned} v_t &= R_1 C_1 \dot{v}_1 + R_1 C_2 \dot{v}_i + R_2 C_2 \dot{v}_i + v_i \\ &= R_1 C_1 \dot{v}_1 + (R_1 + R_2) C_2 \dot{v}_i + v_i. \end{aligned}$$

c. Step 3. Eliminate v_1 and \dot{v}_1 .

$$\begin{aligned} R C_1 \dot{v}_t + v_t &= R_1 C_1 (R C_1 \ddot{v}_1 + \dot{v}_1) + (R_1 + R_2) R C_1 C_2 \ddot{v}_i + \\ &\quad R C_1 \dot{v}_i + (R_1 + R_2) C_2 \dot{v}_i + v_i \\ &= R_1 R_2 C_1 C_2 \ddot{v}_i + (R_1 + R_2) R C_1 C_2 \ddot{v}_i + \\ &\quad (R C_1 + (R_1 + R_2) C_2) \dot{v}_i + v_i \\ &= \underbrace{(R_1 R_2 + R_1 R + R_2 R) C_1 C_2 \ddot{v}_i}_{a} + \\ &\quad \underbrace{(R C_1 + (R_1 + R_2) C_2) \dot{v}_i}_{b} + v_i. \end{aligned}$$

where in the second equality, we used the first equations from *Step 1*. Combining this with equation (B1) we obtain the final relationship.

$$a \ddot{v}_o + b \dot{v}_o + v_o = k (R C_1 \dot{v}_t + v_t). \quad (B5)$$

As a transfer function, we have

$$T(s) = \frac{V_o(s)}{V_t(s)} = k \frac{RC_1 s + 1}{as^2 + bs + 1}. \quad (\text{B6})$$

Note that if $R = 0$, we recover the original Sallen-Key low-pass filter transfer function (2):

$$\frac{V_o(s)}{V_t(s)} = \frac{k}{R_1 R_2 C_1 C_2 s^2 + (R_1 + R_2) C_2 s + 1}.$$

2. Analyzing the circuit

This filter has a zero in the left-half plane at $z = -1/RC_1$, in contrast to the original Sallen-Key filter. The presence of the resistance R is almost always parasitic and does not help with the desired signal generation.

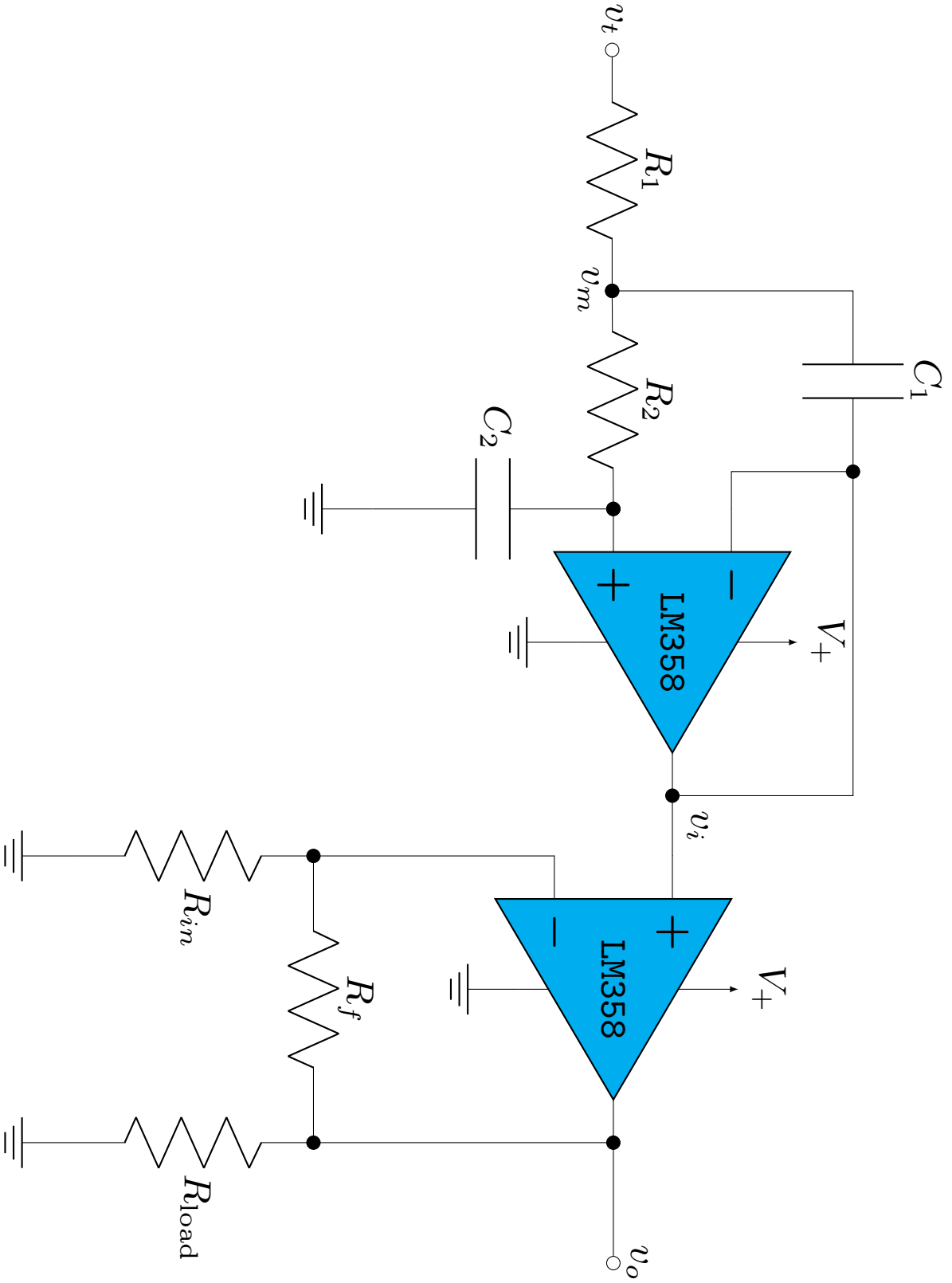


FIG. 9: The final signal generator circuit design.

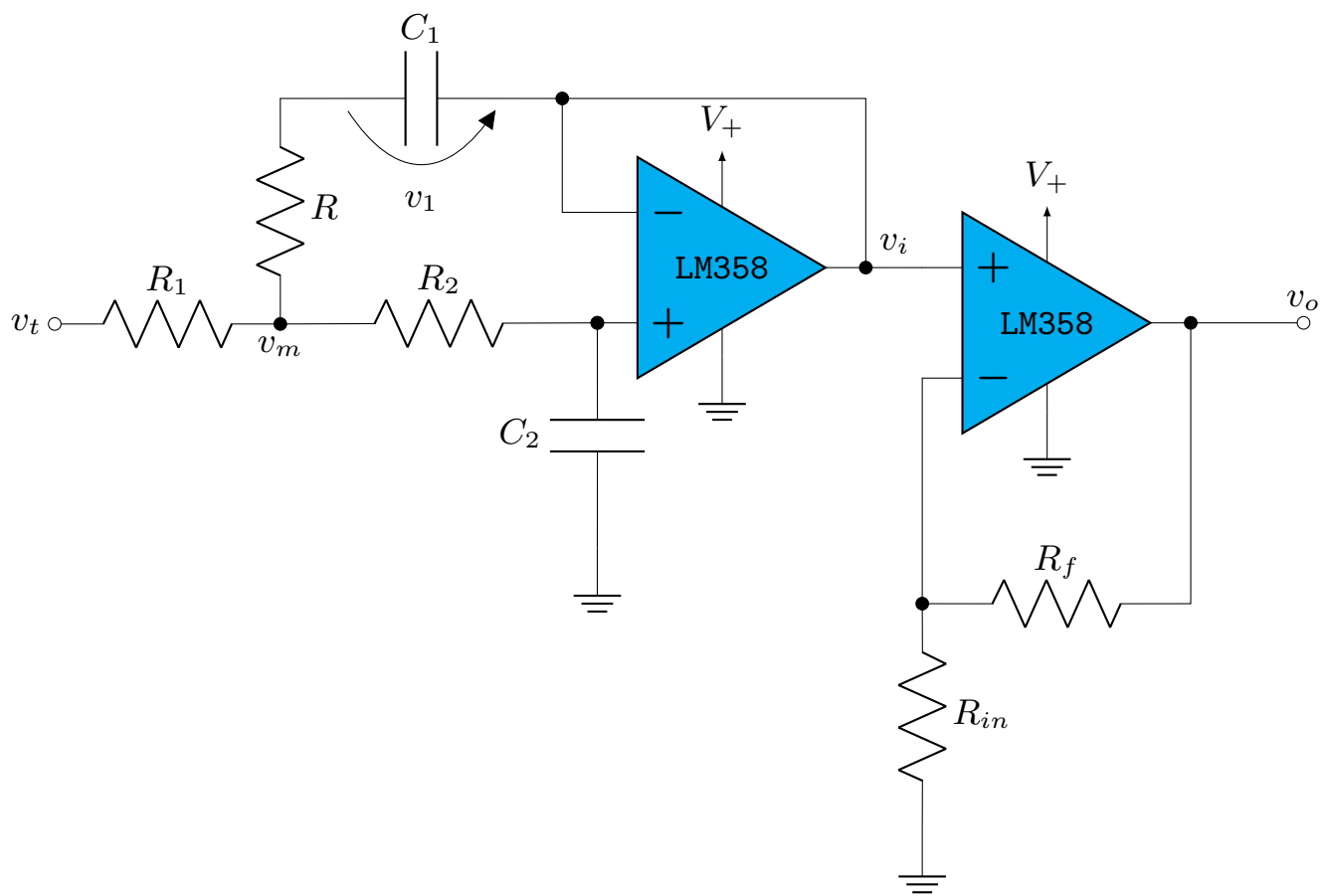


FIG. 10: Alternative LPF circuit.